PHOTONICS Research

Spectrally efficient multi-band visible light communication system based on Nyquist PAM-8 modulation

NAN CHI,* MENGJIE ZHANG, JIANYANG SHI, AND YIHENG ZHAO

Department of Communication Science and Engineering, and Key Laboratory for Information Science of Electromagnetic Waves (MoE), Fudan University, Shanghai 200433, China
**Corresponding author: nanchi@fudan.edu.cn*

Received 26 June 2017; revised 16 September 2017; accepted 18 September 2017; posted 18 September 2017 (Doc. ID 298297); published 20 October 2017

High-speed multi-user access with high spectral efficiency is one of the key challenges for band-limited visible light communication (VLC) systems. In this paper, we propose a novel scheme for effective multiple-access VLC systems based on multi-band, Nyquist-filtered pulse amplitude modulation (PAM)-8 modulation. Within this scenario, the spectral efficiency can be improved from 1.5 to 2.73 b/s/Hz by implementing an appropriate Nyquist filter to suppress spectral bandwidth. We experimentally demonstrate a multi-band VLC system at 1.2 Gb/s after 1 m indoor free space transmission. The system performances have also been thoroughly investigated for different sub-band numbers, utilizing a rectangular filter in the frequency domain and a Nyquist filter based on square root raised cosine. The results show that the Nyquist-filtered PAM-8 signal can outperform a rectangular filtered signal. The maximum improvement of system capacity is up to 1.67 times for the Nyquist-filtered multi-band system. The results clearly show the advantage and feasibility of multi-band Nyquist PAM for high-speed multiple-access VLC systems.

OCIS codes: (060.0060) Fiber optics and optical communications; (060.2605) Free-space optical communication; (230.3670) Light-emitting diodes.

https://doi.org/10.1364/PRJ.5.000588

1. INTRODUCTION

The rapid growth of demand in mobile data traffic has been encouraging researchers to study new radio-access technologies that could be applied to the future fifth-generation (5G) access network. Meanwhile, visible light communication (VLC) based on light-emitting diodes (LEDs) has become an attractive and promising technology for short-range wireless communication, since LEDs can simultaneously provide illumination and communication [1,2]. In comparison to other radio-access technologies, VLC has advantages including being license-free, immune to electromagnetic interference, cost effective, and strong in terms of security. Therefore, VLC is expected to be a potential candidate in next-generation access networks. For the 5G network, one of the key discussions is to support a higher-access data rate with more than 1000 times capacity compared to the current long-term evolution (LTE) system [3]. However, there are several challenges for VLC systems to provide high-speed multi-user access.

On the one hand, the intrinsic modulation bandwidth of commercially available phosphor-based white LED is limited to the several-MHz range [2]. The limited bandwidth of LEDs is one of the main obstacles to high-capacity VLC systems. Thus, the advanced modulation formats have been widely studied and found to provide high spectral efficiency and high data rate access; these formats include orthogonal frequency division multiplexing (OFDM) [4], carrier-less amplitude and phase (CAP) modulation [5], and pulse amplitude modulation (PAM) [6]. Compared with OFDM and CAP modulation, PAM is relatively simple to implement in the real-time domain because PAM, as a one-dimensional modulation, can be directly modulated in intensity. In comparison to OFDM, there is no inverse fast Fourier transform, fast Fourier transform (FFT), or electrical complex-to-real-value conversion required in the PAM system [7]. In addition, compared with OFDM signals, PAM has better resistance to nonlinear behavior due to a lower peak-to-average power ratio [8]. Furthermore, no I/Q separation is required for PAM compared with CAP. Therefore, PAM has attracted extensive attention from researchers due to its simpler structure, lower computational complexity, and more flexible implementation.

Since PAM can only be modulated in one dimension, the spectral efficiency of traditional PAM signals is relatively lower

than CAP and OFDM signals. Thus, some filtering schemes are proposed to compress spectral bandwidth and improve spectral efficiency [9,10]. In Ref. [9], a duobinary filter is employed in a PAM-4 system. The given bandwidth can be reduced by half, but serious inter-symbol interference (ISI) will be introduced by strong filtering to remove the upper part of the spectra. Nyquist filtering based on square root raised cosine is another effective method [10]. Utilizing the filter, the spectral bandwidth can be dynamically adjusted by the roll-off factor. Moreover, the undesired out-of-band power leakage can be effectively mitigated due to the suppression of the side lobes [11].

On the other hand, VLC has traditionally been conceived as a point-to-point cable-replacement technique [2] whereas, from the network point of view, it is desirable for the VLC to have the capability of supporting multiple user access. Therefore, achieving efficient multi-user access is one of the hotspot research topics in VLC systems. Several approaches have been reported for multi-band schemes [12–14]. In Refs. [12,13], the authors demonstrate a multi-band CAP system with spectral efficiency up to 4.85 b/s/Hz by employing an adaptive bit-loading scheme. However, the highest total rate of the multi-band CAP system is only 31.53 Mb/s due to the limited modulation bandwidth of 6.5 MHz, and the transmission rate for these high-index sub-bands is only several MHz. In Ref. [14], multi-band OFDM signals are applied to multiple LED chips to avoid power fading and nonlinearity. However, the scheme may not be cost-efficient, as more users need more LED chips. Additionally, the system is investigated under the modulation bandwidth of 1.95 to 30.27 MHz, so the system can only provide a maximum capacity of 174.8 Mb/s with three sub-bands. These systems are investigated based on a narrow modulation bandwidth. Additionally, the transmission rate is different for each sub-band, since the modulation order selected in each sub-band depends on the measured signal to noise ratio (SNR). But for PAM VLC systems occupying large modulation bandwidth, there is still an absence of investigations to provide multi-band access solutions, as well as assign uniform capacity to each sub-band.

In this paper, we propose a novel multi-band access scheme based on Nyquist PAM-8 modulation to achieve high-speed multi-user access. In this demonstration, the Nyquist filter is utilized to improve spectral efficiency by suppressing spectral bandwidth and out-of-band emissions. Also, weighted pre-equalization [15] is employed to adjust the power allocation of each sub-band and optimize the performance of all sub-bands. At the receiver, scalar modified constant multi-modulus algorithm (S-MCMMA)-based adaptive equalization [16] is employed to eliminate the ISI. For the first time to our knowledge, a multi-band PAM-8 VLC system based on a commercially available red LED is experimentally demonstrated with a data rate up to Gb/s. Total data rates of 1200, 900, 900, 870, and 810 Mb/s can be successfully achieved over 1 m indoor free-space transmission when the sub-band numbers are 2, 3, 4, 5, and 6, respectively. The measured bit error rate (BER) is under the 7% hard decision forward error correction (HD-FEC) limit of 3.8×10^{-3} [17].

Additionally, the system performance is discussed from the aspect of the guard interval, filter parameters, and sub-band numbers. The research indicates that appropriate guard interval can slightly improve system performance. However, it may not be cost efficient for the limited-bandwidth system as larger bandwidth reduces the spectral efficiency. In addition, the roll-off factor of the Nyquist filter is found to be an essential parameter of the system design. By carefully tuning the roll-off factor, the spectral efficiency can be improved from 1.5 to 2.73 b/s/Hz. Then, the system performances utilizing a rectangular filter in the frequency domain and a Nyquist filter are thoroughly investigated for different sub-band numbers. The results show that the Nyquist-filtered PAM-8 signal can significantly outperform a rectangular filtered signal. In comparison to the system utilizing a rectangular filter, the capacities of the Nyquist filtering system with 2, 3, 4, 5, and 6 sub-bands can be improved to be 1.54, 1.54, 1.67, 1.61, and 1.5 times higher, respectively. However, the measured results show that the baud rate will degrade with the increasing of sub-bands, when the modulation bandwidth is close to the limit of the system bandwidth. Therefore, in our future work, the optimal power allocation combined with a bit-loading scheme will be further researched to improve the multi-band system capacity.

2. PRINCIPLE OF MULTI-BAND NYQUIST PAM

Figure 1 shows the schematic diagram of the multi-band Nyquist PAM-8 system. The original bit sequences are first mapped into PAM-8 symbols; then the PAM symbols are up-sampled to match the sample rate of the shaping filters. The sample rate is determined by the modulation bandwidth and the sub-band numbers. Subsequently, the Nyquist filter is applied for pulse generation. The spectral bandwidth and undesired out-of-band power leakage can be effectively suppressed by the filter, and its impulse response in the time domain can be expressed as [18]

$$h(t) = \frac{\sin\left[\pi \frac{t}{T_s}(1-\alpha)\right] + 4\alpha \frac{t}{T_s} \cos\left[\pi \frac{t}{T_s}(1+\alpha)\right]}{\pi \frac{t}{T_s}\left[1 - \left(4\alpha \frac{t}{T_s}\right)^2\right]}, \quad (1)$$

where T_s is the symbol duration and α is the roll-off factor (generally between 0 and 1).

The spectra of the Nyquist and traditional PAM schemes are depicted in Fig. 2. The red line indicates the spectra of the Nyquist PAM and the blue line shows the spectra of traditional PAM. The traditional PAM signals show strong side lobes because the rectangular pulse shaping has sine-shaped response in the frequency domain. Compared with the traditional PAM scheme, the spectral bandwidth and side lobes of the Nyquist PAM scheme can be significantly suppressed by the quasi-square filter. Thus, higher spectral efficiency is successfully obtained. It should be noted that about 50 dB side-lobe attenuation can be achieved in Nyquist PAM, in comparison to the traditional PAM scheme. Therefore, the crosstalk between different sub-bands can be significantly mitigated in the multi-band system based on frequency division multiplexing. In addition, the spectral shape of Nyquist PAM considering different roll-off factors is illustrated in Fig. 3. It can be found that a narrower spectral bandwidth is obtained as the roll-off factor decreases. The spectral bandwidth is controlled by the

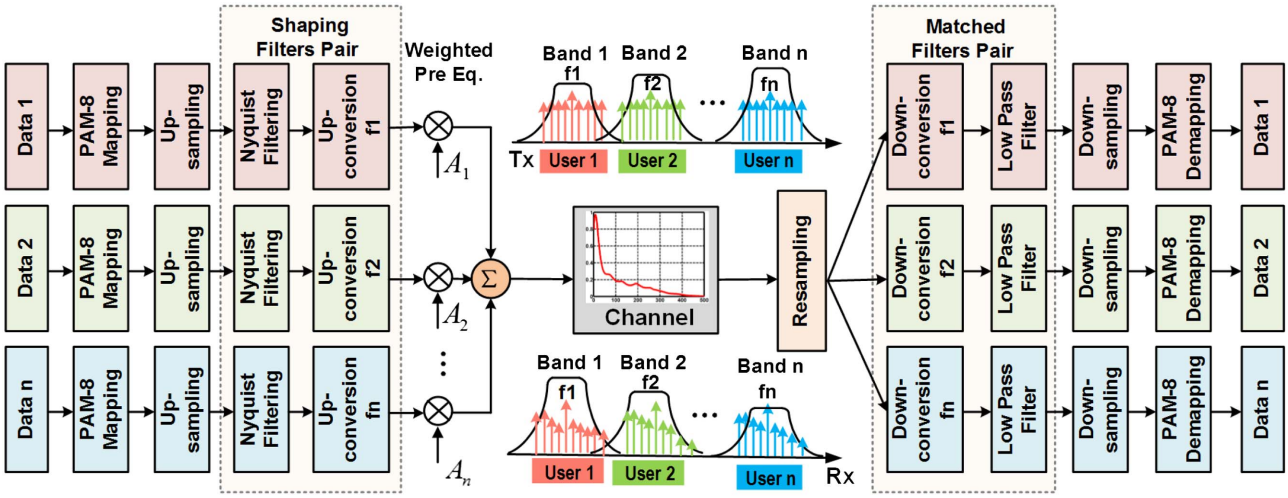

Fig. 1. Schematic diagram of the multi-band Nyquist PAM-8 system.

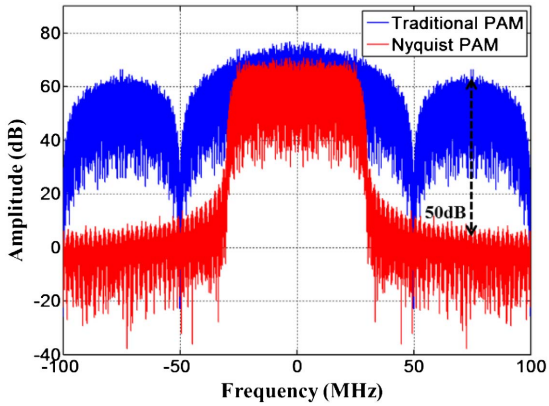

Fig. 2. Spectra of Nyquist PAM compared with traditional PAM.

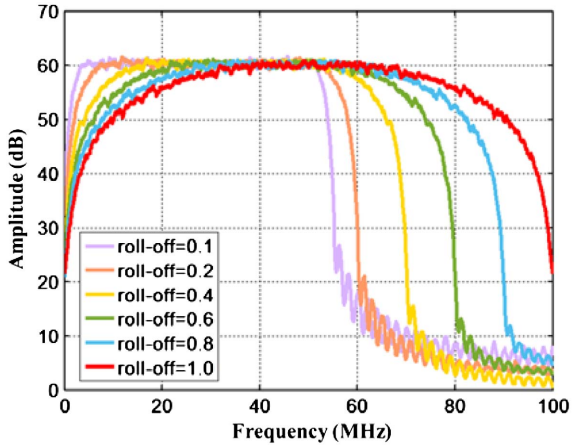

Fig. 3. Spectral shape of Nyquist PAM considering different roll-off factors.

roll-off factor α, and the spectral compression ratio can be expressed as $(1-\alpha)/2$. Although the smaller α can obtain higher spectral efficiency, more serious ISI will be introduced by spectral overlap.

For multiple users, the transmission data of each sub-stream are carried in different subcarrier frequencies by up-conversion. However, the performance of high-frequency sub-bands will seriously deteriorate due to the low SNR induced by high-frequency attenuation. Therefore, a weighted pre-equalization scheme is employed to compensate the frequency attenuation, and the power allocation of each band can be dynamically adjusted to optimize the performances of all sub-bands. In order to reduce the computational complexity, we make a simplification for the weighted pre-equalization scheme proposed in our previous work [15]. There is no need to measure and multiple the reciprocal of the transfer function to compensate for the overall bandwidth, because the attenuation of high-frequency components can be partially compensated by utilizing a self-designed pre-equalizer [19]. The PAM signal of each sub-band is only multiplied by a weighted coefficient A_n to adjust the transmit power of each sub-band. With the increasing of sub-band index n, A_n becomes larger and improves the signal quality carried in high-frequency subcarriers. Finally, the pre-weighted signal of each sub-band is added to form the multi-band signal in the time domain.

In terms of the receiver, the received signal of each band is multiplied by the matched subcarrier frequency and then filtered by low-pass filter (LPF) to split the baseband signal component. After down-sampling, a decoder is utilized to obtain the original bit sequence. In this system, the shaping filter pair consists of the Nyquist filter and up-conversion, and the matched filter pair includes down-conversion and LPF. They are matched to extract the desired sub-band signal from the mixed multi-band signals, thus providing the possibility of application to multi-user access networks.

For a multi-band Nyquist PAM system with N sub-bands, the shaping filter pair in the time domain can be given by [18]

$$h_{fp\_n}(t) = h(t) \cdot \cos(2\pi f_n t), \tag{2}$$

wherein

$$f_n = \frac{(2n-1)(1+\alpha)}{2T_s}. \quad (3)$$

Here, f_n is the subcarrier frequency of the nth sub-band. Assuming $S_n(t)$ is the data carried in the nth sub-band after PAM-8 mapping and up-sampling, A_n is the weighted coefficient for the nth sub-band, so the combined output signals $S(t)$ can be expressed as

$$S(t) = \sum_{n=1}^{N} \left[A_n \cdot (S_n(t) \otimes h_{fp\_n}(t))\right], \quad (4)$$

$$= \sum_{n=1}^{N} [A_n \cdot S'_n(t) \cdot \cos(2\pi f_n t)], \quad (5)$$

where "⊗" is the convolution symbol and $S'_n(t) = S_n(t) \otimes h(t)$ is the Nyquist filtered PAM-8 signal.

After free-space transmission, the received multi-band PAM-8 signal can be expressed as

$$R(t) = \sum_{n=1}^{N} [A_n \cdot S'_n(t) \cdot \cos(2\pi f_n t)] + N_0(t), \quad (6)$$

where $N_0(t)$ is the additive white Gaussian noise. Then the received signal implements down-conversion by multiplying the corresponding subcarrier frequency of each sub-band, so the signal carried in the mth sub-band can be given by

$$R_m(t) = \left\{ \sum_{n=1}^{N} [A_n S'_n(t) \cos(2\pi f_n t)] + N_0(t) \right\} \cdot \cos(2\pi f_m t), \quad (7)$$

$$= A_m S'_m(t) \cos^2(2\pi f_m t) + I_{m,n}(t) + I_N(t), \quad (8)$$

$$= \frac{1}{2} A_m S'_m(t) + \frac{1}{2} A_m S'_m(t) \cos(4\pi f_m t) + I_{m,n}(t) + I_N(t), \quad (9)$$

wherein

$$I_{m,n}(t) = \sum_{n \neq m}^{N} A_n S'_n(t) \cos(2\pi f_n t) \cos(2\pi f_m t), \quad (10)$$

$$I_N(t) = N_0(t) \cos(2\pi f_m t). \quad (11)$$

In Eq. (9), the first term is the PAM signal carried in the mth sub-band. The second term is the second-order intermodulation distortion between symbols located on the mth sub-band. The third term is ICI between the mth sub-band and other sub-bands, as shown in Eq. (10), and the fourth term is the noise signal, as shown in Eq. (11).

Then, the signal is changed to the frequency domain through FFT transform. By passing an LPF, only the first term, including the low-frequency component, can be retained. So the baseband signal for the mth sub-band can be given by

$$R'_m(t) = \frac{1}{2} A_m S'_m(t), \quad (12)$$

and the frequency response for the LPF can be expressed as

$$H(f) = \begin{cases} 1, & |f| \leq \frac{1+\alpha}{2T_s} \\ 0, & |f| > \frac{1+\alpha}{2T_s} \end{cases}, \quad (13)$$

where T_s is the symbol duration and α is the roll-off factor.

3. EXPERIMENTAL SETUP

The experimental setup of the multi-band VLC system based on Nyquist PAM-8 modulation is shown in Fig. 4. The original data sequences are first generated in MATLAB and mapped into PAM-8 symbols. Then, N sets of sequences are up-sampled and filtered by pulse-shaping filters to produce N-band Nyquist PAM-8 signals ($N = 1 - 6$). To compensate for the high-frequency attenuation and optimize the overall performance of the sub-bands, the weighted coefficient is multiplied by each sub-band. Insets (a) and (b) in Fig. 4 show the electrical spectra of the received signal without and with weighted pre-equalization. It can be found that the frequency response of the high-frequency sub-bands can be significantly improved utilizing the weighted pre-equalization. This makes it feasible to load identical modulation orders to each sub-band signal.

In our system, an RGB-LED (LZ4-00MA00, red: 621 nm; green: 525 nm; blue: 460 nm) is utilized as the light source. However, only the red chip is employed to transmit data for two reasons. First, our investigation is mainly focused on the multi-band signal carried in a single wavelength. Second, the frequency response of the red chip is more flat compared with the green and blue chips [20]. Thus, the red chip has larger system bandwidth and more sub-bands can be allocated in the red wavelength. It should be noted that blue and green lights should be simultaneously lighted in practical application so as to form the white light for illuminating.

In the experiment, the generated multi-band PAM signal is fed into an arbitrary waveform generator (AWG, Tektronix AWG710B) and passed through a self-designed bridged-T-based pre-equalizer to compensate for the attenuation of high-frequency components [19]. The bandwidth of the pre-equalizer is 250 MHz. After amplification by a mini-circuits electrical amplifier (EA, mini-circuits, 25-dB gain), the electrical signal and DC-bias voltage are combined by a bias tee and applied to the red chip of the RGB-LED. A reflection cup with 60° divergence angle is applied to the LED to decrease the beam angle. The bias voltage and input signal peak-to-peak value (Vpp) for the red chip is set as 2.1 and 0.3 V, respectively, to ensure the red chip works at the optimal condition [21]. The transmission distance is 1 m.

At the receiver, a commercially available PIN photodiode (Hamamatsu 10784) is used as the receiver; it is equipped with a lens (70 mm diameter and 100 mm focus length) to focus light. The received signal is amplified by an EA and recorded by a digital storage oscilloscope (DSO, Agilent DSO54855A) for further offline signal processing. In offline signal processing, after re-sampling and synchronization, a subcarrier phase-estimation algorithm is employed to correct the subcarrier phase offset, which is introduced by the inconsistent sampling clock between AWG and DSO. The calculated phase offset will be compensated in the matched filter pair to extract each sub-band signal more accurately. After normalization and down-sampling, each sub-band PAM signal is equalized by an

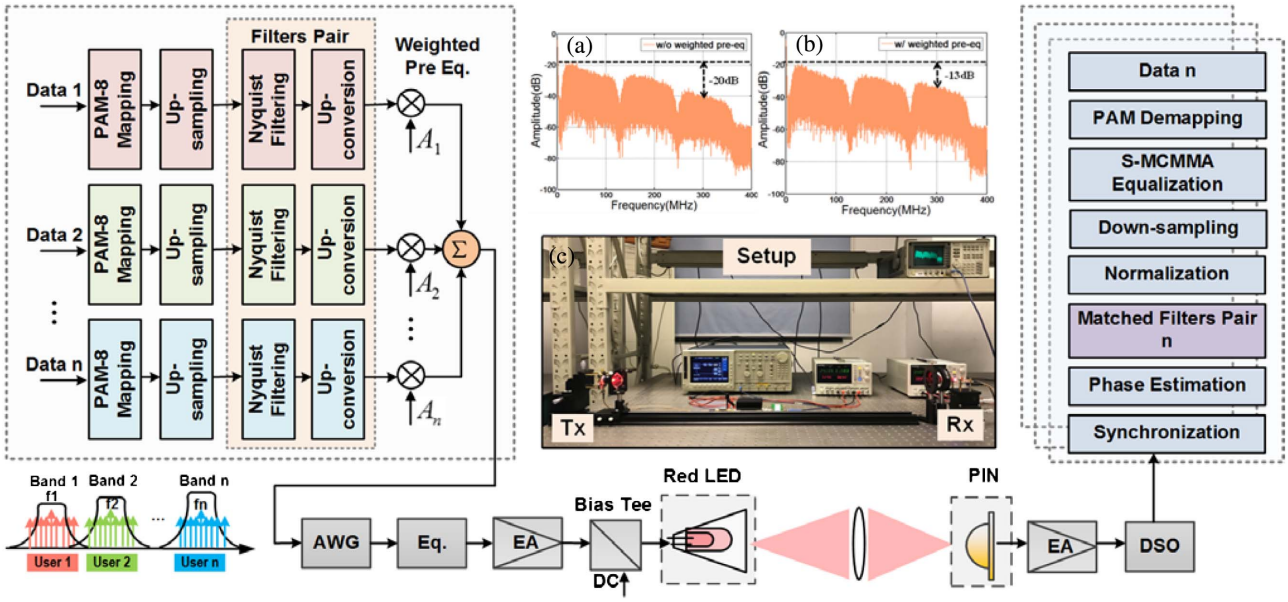

Fig. 4. Experimental setup of the multi-band VLC system based on Nyquist PAM-8 modulation. (a) Measured electrical spectra without weighted pre-equalization; (b) measured electrical spectra with weighted pre-equalization; (c) experimental setup. Eq., pre-equalizer.

S-MCMMA-based adaptive equalizer to eliminate the ISI and compensate for the channel loss [16]. The scheme is a blind post-equalization without any training sequence aiding, so the interaction is required for each symbol; this can be computationally costly depending on the tap number of the equalizer. In our system, the optimal tap number of the S-MCMMA equalizer is set as 21. Finally, the data is decoded to obtain the original bit sequence and calculate the BER.

4. EXPERIMENTAL RESULTS AND DISCUSSION

First, we measured the frequency response of the overall system, including the LED, pre-equalization circuit, EAs, bias tee, and PIN, as shown in Fig. 5. As can be seen, the VLC system is highly band-limited and the −3 dB bandwidth of our system is about 20 MHz, so the high-frequency signal suffers from severe attenuation. By employing pre-equalization,

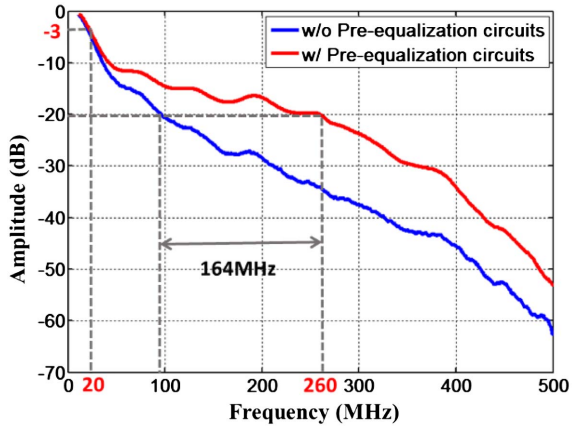

Fig. 5. Measured frequency response of the overall VLC system.

the attenuation can be appropriately compensated and the −20 dB bandwidth of the system can be extended from 96 to 260 MHz.

It is worth noting that the direct current and low-frequency component (less than 10 MHz) are also significantly attenuated due to the limitation of the bias tee. The bias tee used in our experiment is a bandpass device. Thus, we empty out the front bandwidth of 10 MHz, where no signals are carried, to ensure better performance can be obtained.

By pre-equalization, the modulation bandwidth is extended from several tens of MHz to several hundreds of MHz, so higher-speed data can be transmitted in the multi-band VLC system. Then, the system performance based on large modulation bandwidth is investigated from the aspect of the guard interval, filter parameters, and sub-band numbers so as to explore the maximum system capacity of multi-band PAM systems.

A. Guard Interval

In this section, the influence of the guard interval between different sub-bands is investigated. The measured BER performance versus the bandwidth of the guard interval is depicted in Fig. 6. In this demonstration, the baud rate of each sub-band is set as 50 Mbaud. The roll-off factor of the filter is set as 0.2. When no guard band is arranged, three sub-bands are located on the different subcarrier frequencies of 40, 100, and 160 MHz. Then the guard interval increases in steps of 10 MHz, from 0 to 60 MHz. The measured results show that the first sub-band remains the best performer. It can also be demonstrated from the inset that the constellation for the first band is clearer than the other two bands, and the BER performance is stable with the increasing bandwidth of the guard band. However, the performance of the second and third sub-band will first be improved and then deteriorate. This is because the appropriate rising of the guard interval can mitigate

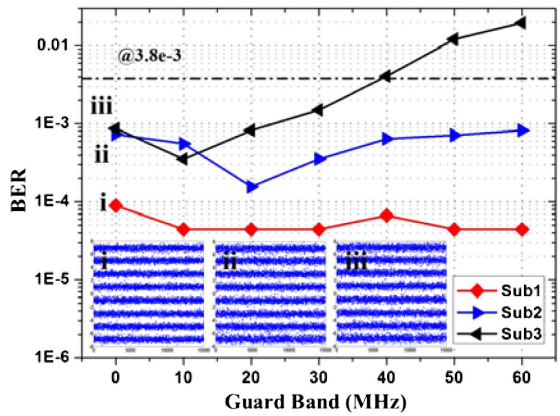

Fig. 6. BER performance versus the bandwidth of the guard band.

the crosstalk between different sub-bands, but the second and third sub-bands will be carried in a higher frequency with the growth of the guard interval. Thus low SNR, induced by the high-frequency attenuation, will become the dominant effect. Additionally, the second sub-band requires larger guard band compared to the other two sub-bands since it suffers more serious crosstalk from both adjacent sub-bands. Therefore, an appropriate guard interval can improve system performance when the bandwidth resources are not considered.

However, for the limited bandwidth system, the guard interval may not be cost-efficient where larger bandwidth is required—especially for when the modulation bandwidth reaches the limit of system bandwidth, as the performance degradation caused by high-frequency attenuation is more serious than inter-band interference. Besides, we want to explore the maximum capacity of the system under limited bandwidth. No guard interval can make full use of bandwidth and improve spectral efficiency. Therefore, no guard interval is considered in our next investigation.

B. Filter Parameters

According to the preceding analysis, the filter is required in PAM systems to improve the spectral efficiency and minimize the crosstalk between different sub-bands, and the spectral compression degree is related to the roll-off factor of the Nyquist filter. Therefore, the filter design is an essential factor affecting the performance of multi-band systems. In this section, we investigate the three-band system performance under different filtering schemes.

The received signal spectra without filters, with the rectangular filter in frequency domain, and with the Nyquist filter at various roll-offs are presented in Fig. 7. The baud rate of each sub-band is set as 50 Mbaud, so the spectral bandwidth of all sub-bands without compression is 300 MHz. It can be seen that the spectra of the received signal without filters suffers serious damage and deformation, in particular for the first band signal. This can be explained by the fact that the original PAM signal has a very high side-lobe component, so the side lobe signal from adjacent sub-bands will be superimposed on the main lobe signal. Therefore, it is necessary to suppress the side lobes by filters in the multi-band system. A common method is to utilize a rectangular filter in the frequency domain to filter out the side lobe component. This is an ideal LPF, which retains the main lobe component of signal spectra completely. However, side-lobe components are entirely suppressed, and thus bandwidth compression cannot be obtained using this filter. The corresponding frequency-domain characteristics can be expressed as

$$H(f) = \begin{cases} 1, & |f| \le \frac{1}{T_s} \\ 0, & |f| > \frac{1}{T_s} \end{cases}, \tag{14}$$

where T_s is the symbol duration.

The measured results show that the spectra with rectangular filter is similar to the spectra with a Nyquist filter at $\alpha = 1$. In both cases, no bandwidth saving can be attained. However, for the Nyquist filter, the bandwidth compression

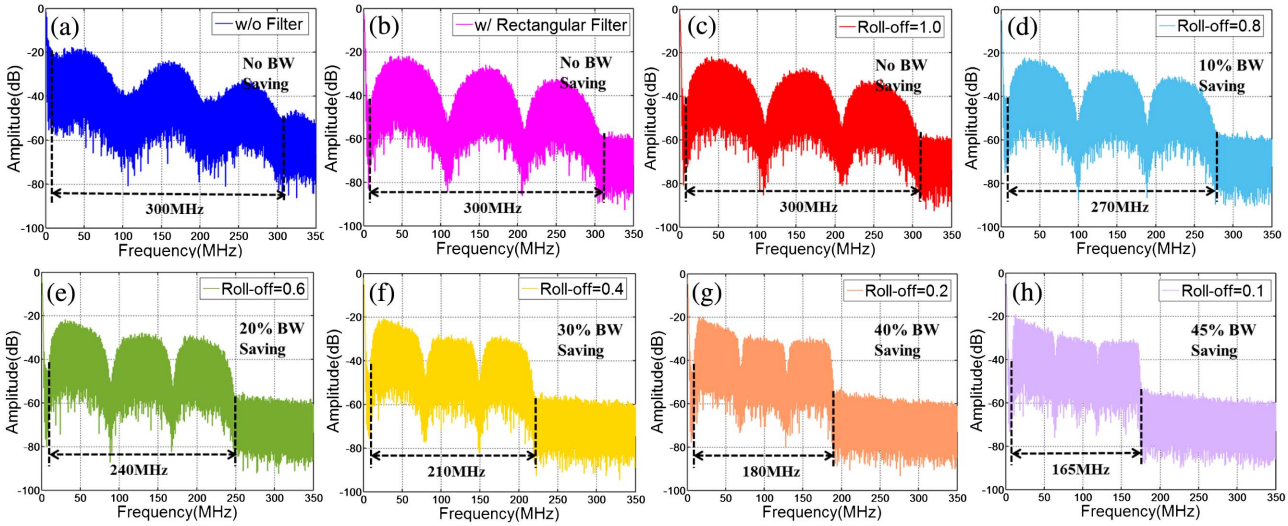

Fig. 7. Measured electrical spectra of received signal (a) without filters, (b) with the rectangular filter in frequency domain, and (c)–(h) with the Nyquist filter at different roll-off factors. BW, bandwidth.

can be successfully achieved by adjusting the roll-off factor. As we can see from Figs. 7(c)–7(h), the bandwidth saving can be improved as the roll-off factor decreases. Meanwhile, the spectral shape gradually changes to square, which is controlled by the impulse response of the filter. However, the interval of different sub-bands decreases, which will introduce interference between adjacent sub-bands.

Additionally, we research the highest transmission rate at different spectral compression degrees to seek out the optimal system capacity, as shown in Fig. 8. Figures 8(a)–8(c) show the BER performance versus different filters for the first, second, and third sub-bands, respectively. As we can see from the blue curve in Figs. 8(a)–8(c), systems without any filter show poor BER performance because severe inter-band interference will be introduced by the unfiltered PAM signal with large side-lobe components. The first sub-band especially suffers stronger low-frequency noise interference, which is from the leaked side-lobe aggregated in the front emptied bandwidth. It can be found that the intensity of the low-frequency noise even exceeds the signal, as shown in Fig. 7(a). Thus, the SNR of the first sub-band is significantly inferior to other sub-bands, and shows the poorest BER performance. However, the performance of the VLC system can be significantly improved by utilizing the filter, and the BER performance of each sub-band can be reduced at least by an order of magnitude.

Then, the system performance is investigated versus different roll-off factors of the Nyquist filter. The measured results show that the highest transmission rate mainly depends on the transmission performance of the third sub-band. Moreover, with the increasing of baud rate, the performance of the sub-band occupying larger bandwidth will seriously degrade due to the high-frequency attenuation induced by limited bandwidth. When the baud rate rises to 100 Mbaud, only the signal with a Nyquist filter at $\alpha = 0.2$ can render all sub-bands able to reach the BER threshold. In this case, the data rate of each sub-band is 300 Mb/s, so the aggregated data rate of 900 Mb/s for the three-band system can be achieved with the BER under the 7% FEC limit of 3.8×10^{-3}. Compared with the system utilizing a rectangular filter, the system capacity has been increased by 53.85%. Moreover, a 40% bandwidth saving is successfully achieved by the spectral suppression.

The highest baud rate and spectral efficiency achieved for the system utilizing a Nyquist filter is demonstrated in Fig. 8(d) for different roll-off factors. The measured result shows that the spectral efficiency gradually increases as the roll-off factor decreases. By carefully turning the roll-off factor, the spectral efficiency can be improved from 1.5 to 2.73 b/s/Hz. However, the optimal transmission rate of 100 Mbaud with a spectral efficiency of 2.5 b/s/Hz is obtained at $\alpha = 0.2$. When α is more than 0.2, the baud rate is gradually degraded as

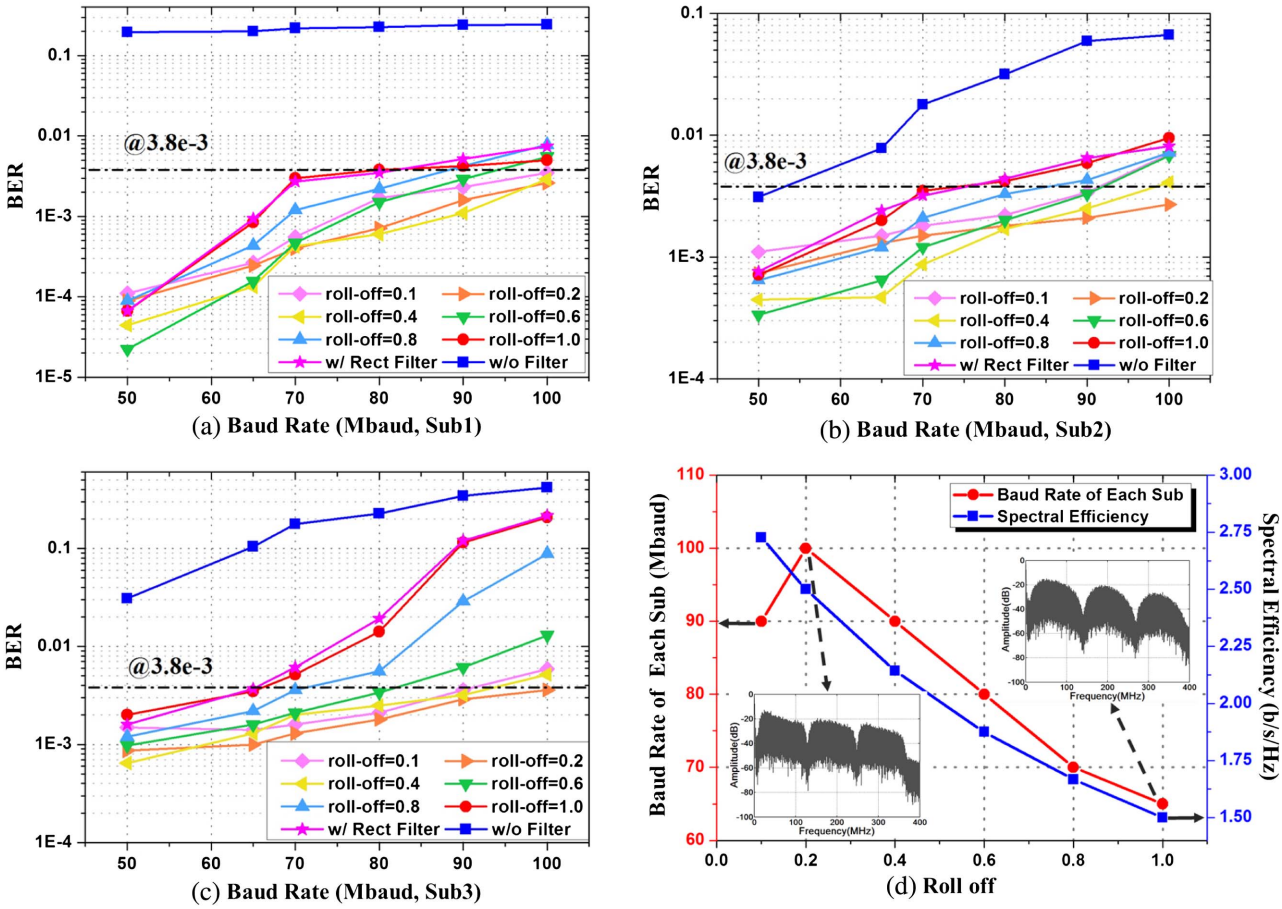

Fig. 8. Measured results: (a)–(c) BER performance versus different filters for sub-bands 1–3. (d) Highest baud rate and spectral efficiency achieved for the system utilizing Nyquist filter with different roll-off factors.

the roll-off factor increases. This can be explained by the fact that a larger occupied bandwidth is required, so the signal carried in high frequency is seriously attenuated due to the limited bandwidth of the LED. As shown in the insets, the bandwidth of 100 Mbaud signal at $\alpha = 0.2$ is 360 MHz, while the bandwidth of 65 Mbaud signal at $\alpha = 1$ is 390 MHz. However, smaller roll-off will decrease the interval between adjacent sub-bands, which induces more serious ICI. When less bandwidth is occupied, the ICI becomes the dominant effect on system performance. It can be verified that the system capacity at $\alpha = 0.1$ is slightly inferior to the capacity at $\alpha = 0.2$. Therefore, the system performance is the compromise between the spectral compression and ICI. The system capacity can be significantly improved by appropriately decreasing the roll-off factor, but too small a roll-off factor will also degrade performance. According to the measured results, 0.2 is the optimal roll-off factor for our system.

C. Sub-Band Numbers

In order to support more multi-user access, the system performance versus different sub-band numbers is discussed. The received spectra with $N = 1$, 2, 3, 4, 5, and 6 sub-bands is illustrated in Fig. 9. In this demonstration, the roll-off factor is 0.2 and the overall spectral bandwidth is fixed at 288 MHz. Thus, the baud rates of each sub-band are set as follows: 240, 120, 80, 60, 48, and 40 Mbaud for sub-band number $N = 1$, 2, 3, 4, 5, and 6, respectively. The measured results show that the high-frequency component of the 1-sub system suffers from the most obvious attenuation. However, when the sub-band number increases, the high-frequency attenuation can be gradually mitigated. Since more sub-bands are allocated, the smaller bandwidth is occupied by each sub-band. Thus, the frequency-dependent attenuation is minimized. Additionally, the weighted coefficient of each sub can be adjusted to allow more power to be allocated to sub-bands with low SNR.

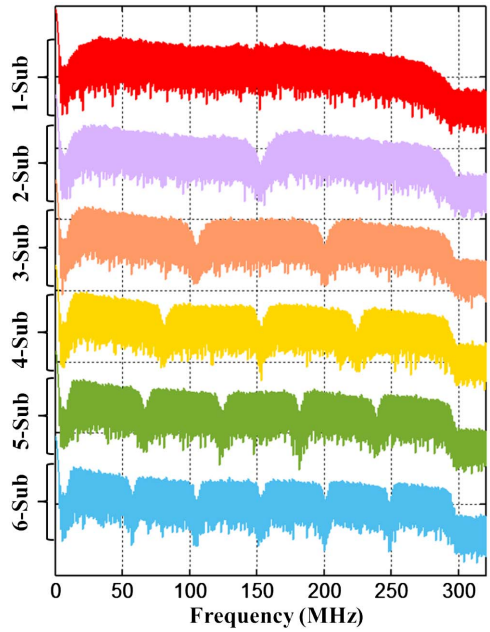

Fig. 9. Measured electrical spectra with $N = 1$ – 6 sub-bands.

Consequently, a more identical frequency response for each sub-band can be obtained in the multi-band system.

The BER performance of each sub-band versus different sub-band numbers is also measured, as depicted in Fig. 10. It can be found that the BER performance of the low subcarrier index deteriorates with the increasing number of sub-bands. However, for the high subcarrier index, the BER performance can be improved slightly as the result of transmitting power distribution induced by the adjustment of the weighted coefficient. The SNR of sub-bands carried in high frequency enhanced for higher transmit power is assigned to compensate for high-frequency attenuation. However, the total transmitting power is constant, so the power allocated to the low-index sub-band will be reduced to the maximum extent within its allowable range. In addition, the degradation of overall BER performance is caused by the more serious ICI introduced by the smaller interval between sub-bands. However, the BER performance of each sub-band tends to be uniform with the increase of sub-bands. The insets show the constellation diagrams of the first sub-band signal located on the 2, 4, 5, and 6 sub-band systems, respectively. It can be found that constellations deteriorate with the increasing of sub-bands. The BERs for these four signals are 1.34×10^{-4}, 7.56×10^{-4}, 1×10^{-3}, and 1.6×10^{-3}, respectively.

Then we research the total capacity of the multi-band system with Nyquist filter and rectangular filter in the frequency domain, versus different sub-band numbers, as shown in Fig. 11. Here, the solid line represents the total baud rate of the system and the dashed line shows the baud rate of each sub-band. It can be found that the system capacity can be significantly improved using the Nyquist filter as opposed to the rectangular filter. For the system with the Nyquist filter, the baud rate of each sub for 1, 2, 3, 4, 5, and 6 sub-bands are 400, 200, 100, 75, 58, and 45 Mbaud, respectively. Namely, the aggregate bit rate is 1200, 1200, 900, 900, 870, and 810 Mb/s, so the maximum system capacity of 1.2 Gb/s is successfully achieved in the 1 and 2 sub-band system based on Nyquist filtering. However, the baud rate of each sub-band with the rectangular filter is 300, 130, 65, 45, 36, and 30 Mbaud for 1, 2, 3, 4, 5, and 6 sub-bands, respectively. Thus, by employing the Nyquist filter, a capacity improvement

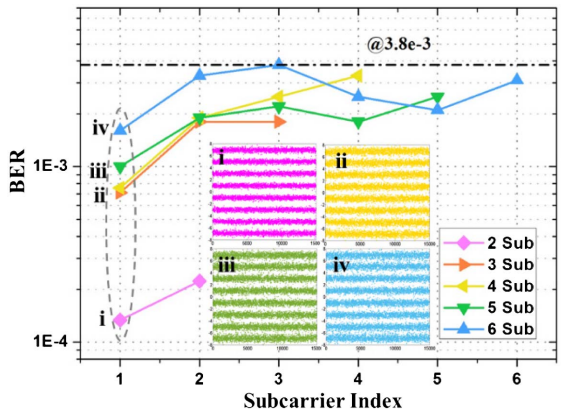

Fig. 10. Measured BER performance of each sub-band for different numbers of sub-bands.

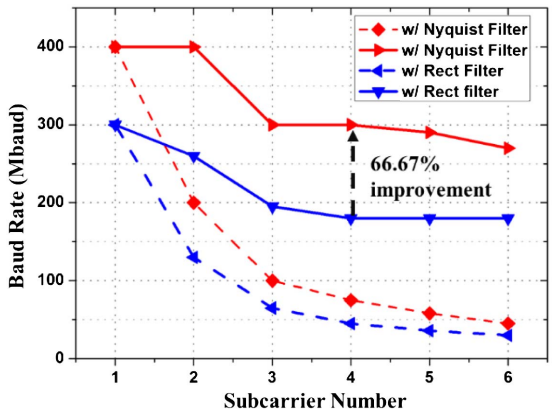

Fig. 11. Total capacity of multi-band system for different numbers of sub-bands.

of 1.33, 1.54, 1.54, 1.67, 1.61, and 1.5 times can be successfully obtained for the 1, 2, 3, 4, 5, and 6 sub-band systems, respectively.

However, the measured results indicate that the baud rate of each sub-band will degrade with the increasing of sub-band numbers. When sub-bands increase from 2 to 3, the system total capacity significantly decreases. As sub-bands continue to grow, the decrease of system capacity becomes slight. The decreasing of system capacity can be explained for two reasons. First, more serious crosstalk between adjacent sub-bands is introduced by the increase in sub-bands. Second, the modulation order for each sub-band is fixed as 8. With the increasing of sub-bands, the average SNR of the high-index sub-band will degrade due to serious high-frequency attenuation. The low SNR cannot support the transmission of signal with high-order modulation, and thus the BER performance significantly deteriorates and cannot reach the FEC threshold. However, the performance of the overall system mainly depends on those sub-bands with poor BER performance, so the overall system capacity is decreased. Although the SNR deterioration for high-index sub-bands can be compensated by adjusting the transmitting power, it is still limited considering the overall power contribution. Therefore, in our future work, the bit-loading scheme combined with power allocation for multi-band signals will be further researched to improve the system capacity.

Additionally, it should be noted that the luminance of the LED is one of the key factors that limit the transmission distance in the VLC system. In our experiment, the output power of the LED is below 2.5 W and the luminance measured at 1 m is 129 lx, which is far below the standard value for brightness (500 lx). The luminance decreasing with distance will reduce the system transmission capacity. Thus, the system performance and transmission distance can be further improved by deploying several LED chips together to increase luminance. Besides, the signal can be carried in several LED chips by wavelength division multiplexing, so the system capacity and degree of multi-user access can also be greatly enhanced.

5. CONCLUSION

In this paper, for the first time to our knowledge, we experimentally demonstrate a high-speed multi-band VLC system based on Nyquist PAM-8 modulation with one red LED. In this demonstration, the Nyquist filter is utilized in the pulse-shaping of each sub-band to improve spectral efficiency and mitigate the out-of-band power leakage. Meanwhile, weighted pre-equalization is employed to compensate for high-frequency attenuation and adjust the power allocation of each sub-band. The system performance based on large modulation bandwidth is investigated from the aspect of the guard interval, filter parameters, and sub-band numbers. The measured results show that the optimal performance can be achieved at the 40% bandwidth saving due to the compromise between spectral compression and crosstalk in different sub-bands. Moreover, in 1 m indoor free-space transmission, the aggregate transmission rates of 1200, 1200, 900, 900, 870, and 810 Mb/s can be successfully achieved with the BER under 7% FEC limit of 3.8×10^{-3} for the 1, 2, 3, 4, 5, and 6 sub-band systems, respectively. The system performance utilizing a rectangular filter in the frequency domain and a Nyquist filter have also been thoroughly investigated for different numbers of sub-bands. The results show that the Nyquist-filtered PAM-8 signal can significantly outperform the rectangular filtered signal. In comparison to the system utilizing the rectangular filter, the maximum improvement of system capacity is up to 1.67 times for the Nyquist-filtered multi-band system. The measured results clearly demonstrate the advantage and feasibility of multi-band Nyquist PAM modulation for high-speed multi-user-access VLC systems.

Funding. National Key Research and Development Program of China (2017YFB0403603).

REFERENCES

1. D. O'Brien, H. L. Minh, L. Zeng, G. Faulkner, K. Lee, D. Jung, Y. Oh, and E. T. Won, "Indoor visible light communications: challenges and prospects," Proc. SPIE **7091**, 709106 (2008).
2. N. Chi, H. Haas, M. Kavehrad, T. D. Little, and X. L. Huang, "Visible light communications: demand factors, benefits, and opportunities," IEEE Wireless Commun. **22**, 5–7 (2015).
3. J. Zhang, J. Wang, M. Xu, F. Lu, L. Cheng, J. Yu, and G.-K. Chang, "Full-duplex asynchronous quasi-gapless carrier-aggregation using filter-bank multi-carrier in MMW radio-over-fiber heterogeneous mobile access networks," in *Optical Fiber Communication Conference*, OSA Technical Digest (online) (Optical Society of America, 2016), paper Tu-2B.2.
4. H. Elgala, R. Mesleh, and H. Haas, "Indoor broadcasting via white LEDs and OFDM," IEEE Trans. Consum. Electron. **55**, 1127–1134 (2009).
5. F. Wu, C. Lin, C. Wei, C. Chen, Z. Chen, and H. Huang, "3.22-Gb/s WDM visible light communication of a single RGB LED employing carrier-less amplitude and phase modulation," in *Optical Fiber Communication Conference*, OSA Technical Digest (online) (Optical Society of America, 2013), paper OTh1G.4.
6. G. Stepniak, L. Maksymiuk, and J. Siuzdak, "1.1 Gbit/s white lighting LED-based visible light link with pulse amplitude modulation and volterra DFE equalization," Microw. Opt. Technol. Lett. **57**, 1620–1622 (2015).
7. L. Tao, Y. Wang, Y. Gao, A. P. T. Lau, N. Chi, and C. Lu, "Experimental demonstration of 10 Gb/s multi-level carrier-less amplitude and phase modulation for short range optical communication systems," Opt. Express **21**, 6459–6465 (2013).
8. G. Stepniak, L. Maksymiuk, and J. Siuzdak, "Experimental comparison of PAM, CAP, and DMT modulations in phosphorescent white LED transmission link," IEEE Photon. J. **7**, 1–8 (2015).

9. L. F. Suhr, J. V. Olmos, and I. T. Monroy, "10-Gbps duobinary-4-PAM for high-performance access networks," in *Asia Communications and Photonics Conference 2014*, OSA Technical Digest (online) (Optical Society of America, 2014), paper ATh3A-161.
10. M. Zhang, M. Shi, F. Wang, J. Zhao, Y. Zhou, Z. Wang, and N. Chi, "4.05-Gb/s RGB LED-based VLC system utilizing PS-Manchester coded Nyquist PAM-8 modulation and hybrid time-frequency domain equalization," in *Optical Fiber Communication Conference*, OSA Technical Digest (online) (Optical Society of America, 2017), paper W2A.42.
11. M. Xu, J. Zhang, F. Lu, J. Wang, L. Cheng, M. I. Khalil, D. Guidotti, and G. Chang, "Orthogonal multiband CAP modulation based on offset-QAM and advanced filter design in spectral efficient MMW RoF systems," J. Lightwave Technol. **35**, 997–1005 (2017).
12. P. A. Haigh, S. T. Le, S. Zvanovec, Z. Ghassemlooy, P. Luo, T. Xu, P. Chvojka, T. Kanesan, E. Giacoumidis, P. Canyelles-Pericas, H. L. Mihn, W. Popoola, S. Rajbandari, I. Papakonstantinou, and I. Darwazeh, "Multi-band carrier-less amplitude and phase modulation for bandlimited visible light communications systems," IEEE Wireless Commun. **22**, 46–53 (2015).
13. P. A. Haigh, A. Burton, K. Werfli, H. L. Minh, E. Bentley, P. Chvojka, W. O. Popoola, I. Papakonstantinous, and S. Zvanovec, "A multi-CAP visible-light communications system with 4.85-b/s/Hz spectral efficiency," IEEE J. Sel. Areas Commun. **33**, 1771–1779 (2015).
14. C. H. Yeh, H. Y. Chen, C. W. Chow, and Y. L. Liu, "Utilization of multi-band OFDM modulation to increase traffic rate of phosphor-LED wireless VLC," Opt. Express **23**, 1133–1138 (2015).
15. Y. Wang, L. Tao, Y. Wang, and N. Chi, "High speed WDM VLC system based on multi-band CAP64 with weighted pre-equalization and modified CMMA based post-equalization," IEEE Commun. Lett. **18**, 1719–1722 (2014).
16. M. Zhang, Y. Wang, Z. Wang, J. Zhao, and N. Chi, "A novel scalar MCMMA blind equalization utilized in 8-PAM LED based visible light communication system," in *IEEE International Conference on Communications Workshops (ICC)* (2016), pp. 321–325.
17. A. Leven, F. Vacondio, L. Schmalen, S. Brink, and W. Idler, "Estimation of soft FEC performance in optical transmission experiments," IEEE Photon. Technol. Lett. **23**, 1547–1549 (2011).
18. J. Zhang, J. Yu, F. Li, N. Chi, Z. Dong, and X. Li, "$11 \times 5 \times 9.3$ Gb/s WDM-CAP-PON based on optical single-side band multi-level multi-band carrier-less amplitude and phase modulation with direct detection," Opt. Express **21**, 18842–18848 (2013).
19. X. Huang, J. Shi, J. Li, Y. Wang, Y. Wang, and N. Chi, "750Mbit/s visible light communications employing 64QAM-OFDM based on amplitude equalization circuit," in *Optical Fiber Communication Conference*, OSA Technical Digest (online) (Optical Society of America, 2015), paper Tu2G.1.
20. Y. Wang, X. Huang, L. Tao, J. Shi, and N. Chi, "4.5-Gb/s RGB-LED based WDM visible light communication system employing CAP modulation and RLS based adaptive equalization," Opt. Express **23**, 13626–13633 (2015).
21. N. Chi, M. Zhang, Y. Zhou, and J. Zhao, "3.375-Gb/s RGB-LED based WDM visible light communication system employing PAM-8 modulation with phase shifted Manchester coding," Opt. Express **24**, 21663–21673 (2016).